frontiers | Frontiers in Earth Science

TYPE Original Research
PUBLISHED 09 February 2023
DOI 10.3389/feart.2023.1130070

OPEN ACCESS

EDITED BY
Zizheng Guo,
Hebei University of Technology, China

REVIEWED BY
Jingzhe Chen,
Shanghai University, China
Le Wang,
China Jiliang University, China

*CORRESPONDENCE
Wenfeng Wang,
wangwenfeng@sit.edu.cn
Xi Chen,
cx@ms.xjb.ac.cn

SPECIALTY SECTION
This article was submitted to Environmental Informatics and Remote Sensing, a section of the journal Frontiers in Earth Science

RECEIVED 22 December 2022
ACCEPTED 30 January 2023
PUBLISHED 09 February 2023

CITATION
An P, Wang W, Chen X, Zhuang Z and Cui L (2023), Machine learning brings new insights for reducing salinization disaster. *Front. Earth Sci.* 11:1130070. doi: 10.3389/feart.2023.1130070

Machine learning brings new insights for reducing salinization disaster

Peng An[1], Wenfeng Wang[1,2,3]*, Xi Chen[3,4,5,6]*, Zhikai Zhuang[7] and Lujie Cui[2]

[1]Ningbo University of Technology, Ningbo, China, [2]Shanghai Institute of Technology, Shanghai, China, [3]Xinjiang Institute of Ecology and Geography, Chinese Academy of Sciences, Urumqi, China, [4]University of Chinese Academy of Sciences, Beijing, China, [5]Sino-Belgian Joint Laboratory of Geo-Information, Urumqi, China, [6]CAS Research Centre for Ecology and Environment of Central Asia, Urumqi, China, [7]The University of Hong Kong, Hong Kong, China

This study constructs a machine learning system to examine the predictors of soil salinity in deserts. We conclude that soil humidity and subterranean CO_2 concentration are two leading controls of soil salinity—respectively explain 71.33%, 13.83% in the data. The (R^2, root-mean-square error, RPD) values at the training stage, validation stage and testing stage are (0.9924, 0.0123, and 8.282), (0.9931, 0.0872, and 7.0918), (0.9826, 0.1079, and 6.0418), respectively. Based on the underlining mechanisms, we conjecture that subterranean CO_2 sequestration could reduce salinization disaster in deserts.

KEYWORDS

salinization disaster, principal components analysis (PCA), artificial neural network (ANN), long short-term memory (LSTM), subterranean CO_2 sequestration

1 Introduction

Soil salinization is one major type of land desertification and degradation in the world, which is a disaster to global resources and ecology (Dehaan and Taylor, 2002; Metternicht and Zinck, 2008; Li et al., 2014; Singh, 2015; Savich et al., 2021). Such disaster not only brought great impact and serious losses to food production, but also hindered the sustainable development of agriculture (Kotb et al., 2000; Amezketa, 2006; Rengasamy, 2016; Okur and Örçen, 2020; Hassani et al., 2021). The influences of soil salinization disaster to other aspects of society and economy are also inevitable (Schofield et al., 2001; Ghollarata and Raiesi, 2007; Ding et al., 2011; Wang and Li, 2013; Nachshon, 2018; Yang et al., 2020). The disaster leads to a low rate of soil utilization and a sharp decline of forests (De Pascale et al., 2005; Li-Xian et al., 2007; Xiaohou et al., 2008; Bouksila et al., 2013; Wu et al., 2014; Teh and Koh, 2016; Zhou et al., 2017; Li et al., 2018; Zhuang et al., 2022). Ecologists have made great efforts to develop theory and methodology for reducing soil salinization disaster (Lavado and Taboada, 1987; El Harti et al., 2016; Wang et al., 2019). But until now, the degree of global soil salinization is still increasing (Tian and Zhou, 2000; Aragüés et al., 2015; Jesus et al., 2015).

Considering its threats to the earth environments, any theory and methodology for reducing soil salinization disaster is worthy to be discussed (Welle and Mauter, 2017). In the era of artificial intelligence, machine learning has been introduced in the frontier of earth science (Jiang et al., 2018; Huang et al., 2020a; Huang et al., 2020b; Chang et al., 2020; Huang et al., 2020c). The machine learning system is mainly composed of input layer, output layer and hidden layers (Chahal and Gulia, 2019). After obtaining a training set, the learning system can extract effective features (LeCun et al., 2015). These features are connected by artificial neurons (Hao et al., 2016). The neurons receive data from the input layer, make computation with

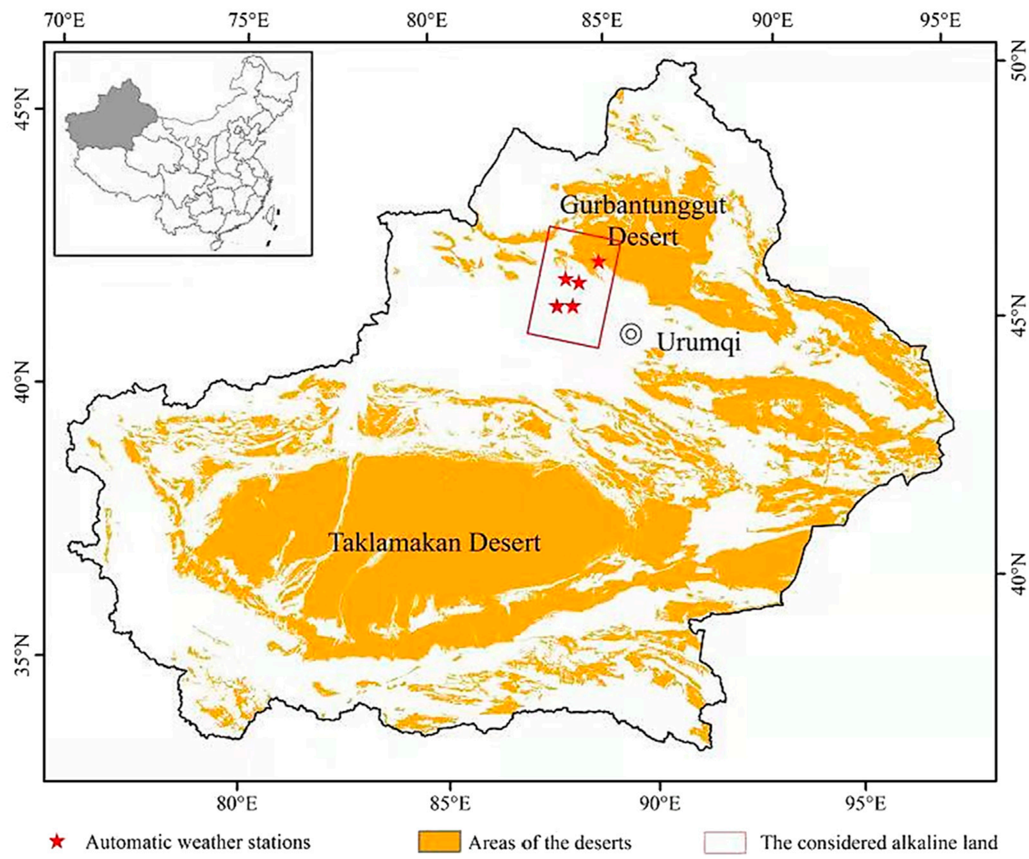

FIGURE 1
Spatial distribution of the five automatic monitoring stations where the meteorological, soil and subterranean data are collected for the present study.

assigned weights—passed through the activation function in the hidden layers, and finally work out the results in the output layer (Coşkun et al., 2017). By testing the trained network, we can assess the errors between the outputs and correct results (Kato et al., 2016). Some latest researches constructed 3-stages learning systems (the training stage, validation stage and testing stage) to improve the generalization capability (Gatos et al., 2019; Skrede et al., 2020; Zhuang et al., 2021).

Our objectives of this study are 1) to construct a machine learning system and examine the predictors of soil salinity in a desert by this learning system, 2) to evaluate the most interpretable proportion of the leading predictors, which will highlight the unneglectable contribution of the subterranean CO_2 concentration to soil salinity, and 3) to analyze the underlining mechanisms for such contribution and according to these mechanisms, to present new insights for reducing salinization disaster in deserts. The organization of the whole paper is as follows. In Section 2, we will construct the machine learning system for examining the predictors, along with some preliminaries and the driven data. Principal components analysis (PCA) is integrated with the artificial neural network (ANN) and long-short term memory (LSTM). Performance of PCA-ANN-LSTM will be presented and the leading predictors will be determined in Section 3. We will also assess the largest proportion of two leading predictors in explaining soil salinity and further clarify their leading roles. Based on the results from PCA-ANN-LSTM calibrations, in Section 4, some new insights will be expanded for reducing soil salinization disaster and the underlining mechanisms will be theoretically analyzed. The conclusions and next research priorities are presented in Section 5.

2 The machine learning system

2.1 The learning mechanisms

The learning mechanisms depend on not only the problem itself but also the components of the data. As stated in Section 1, the considered problem is to construct a machine learning system for examining the potential predictors of soil salinity in a desert by this learning system. That is, the input data of the system is environmental variables (meteorological, soil, and subterranean factors), while the output data is soil salinity. These data were collected from the Manas River Basin of Xinjiang Uygur autonomous region, which is located at the southern periphery of the Gubantonggut Desert, China, as shown in Figure 1. We established five stations by integrating 13 sensors to collect the meteorological, soil and subterranean data, including the CO_2 concentration 3 m beneath the soil (Cs) and 10 cm above the soil (Ca), the soil temperature (Ts), humidity (Hs), alkalinity (pH) and salinity (Y) at 10 cm depth, the atmospheric temperature (Ta), humidity (Ha), air pressure (AP), wind speed (WS), wind direction (WD), rainfall (R), and groundwater level (WL). In order to develop a novel deep neural network to detect the potential environmental controls of soil salinity, Y is employed as the dependent variable of the network and the other 12 environmental factors are naturally employed as independent variables. The basic learning mechanisms of a neural network can be described as follows. The neuron input x was calculated from the model established in (Zhuang et al., 2021).

Alternatively, we integrated the principal component analysis (PCA) and the artificial neural network (ANN) to examine the potential control of Cs, where PCA was improved by the singular value decomposition (SVD) (Van Loan, 1976; Klema and Laub, 1980; Paige and Saunders, 1981; Mandel, 1982; Stewart, 1993). Suppose Θ^i is the weight matrix and $g(x)$ is the activation function. Let $z^{(j)}$ be the pulses to the jth layer, which results in $a^{(j)}$. Let $h_\theta(x)$ be the result in the output layer.

That is,

$$z^{(j)} = \Theta^{(j)} a^{(j-1)}, a^{(j)} = g\left(z^{(j)}\right) \tag{1}$$

Hence the learning mechanisms can be formulated as

$$\begin{bmatrix} x_0 \\ x_1 \\ x_2 \\ \cdots \end{bmatrix} \rightarrow \begin{bmatrix} a_0^{(1)} \\ a_1^{(1)} \\ a_2^{(1)} \\ \cdots \end{bmatrix} \rightarrow \begin{bmatrix} a_0^{(2)} \\ a_1^{(2)} \\ a_2^{(2)} \\ \cdots \end{bmatrix} \rightarrow \begin{bmatrix} a_0^{(3)} \\ a_1^{(3)} \\ a_2^{(3)} \\ \cdots \end{bmatrix} \rightarrow \cdots \rightarrow \begin{bmatrix} a_0^{(j)} \\ a_1^{(j)} \\ a_2^{(j)} \\ \cdots \end{bmatrix} \rightarrow \begin{bmatrix} h_\theta(x)_1 \\ h_\theta(x)_2 \\ h_\theta(x)_3 \\ \cdots \end{bmatrix} \tag{2}$$

and

$$h_\theta(x) = \begin{bmatrix} h_\theta(x)_1 \\ h_\theta(x)_2 \\ h_\theta(x)_3 \\ \cdots \end{bmatrix} = a^{(j)} \tag{3}$$

where the backpropagation process is monitored by the loss function

$$J(\Theta) = -\frac{1}{m}\sum \left(Y^T .* log\left(h_\theta(x)\right) .* \left(1 - Y^T\right)\right) \tag{4}$$

2.2 The learning processes

Differing from (Zhuang et al., 2021), we further introduce a brain-inspired mechanism in the learning processes. That is, we further improve SVD-PCA-ANN by long-short-memory neural network (LSTM) (Salman et al., 2018; Ali et al., 2020; Ahmad and Zhang, 2022; Gao, 2022; Rusnac and Grigore, 2022) and proposed a novel deep neural network PCA-ANN-LSTM to detect the potential environmental controls of soil salinity in the desert. The output of the SVD-PCA-ANN will not be directly input into LSTM. Instead, we utilize the errors data of the SVD-PCA-ANN model as the input data of LSTM. That is, we employ LSTM for learning and reducing the errors to improve the robustness when detecting the potential environmental controls of soil salinity and analyzing the contributions of the subterranean CO_2 concentration to the soil salinity.

The necessity to further integrate with LSTM in the learning processes can be explained as follows. In ANN, it is assumed that the output only depends on the current input, which is not true in the real world (Gu et al., 2019). LSTM allows us to infer the potential relationships among the content of the context, because it is a recurrent neural network (RNN)—the output depends on the current input and memory (Klimov et al., 2020; Huang et al., 2021; Li et al., 2022; Gorgij et al., 2023). The basic idea of RNN is to build a hidden state for acquiring the information at the previous time point and the global parameters are calculated from the current time and all previous memories. Each cell in RNN shares these parameters to reduce the amount of calculation. For LSTM, the current input is linked with the state of the hidden layers in the previous time through three gates—the input gate (information adding), forgetting gate (information discarding) and output gate (Robinson and Zaffaroni, 1997).

A sketch of the learning processes is shown in Figure 2, which construct cells in the machine brain (O'Doherty et al., 2011; Wang et al., 2020; Wang et al., 2021; Wang et al., 2022). We can understand the LSTM learning process with the cells' states. For a cell state C_{t-1} with the input x_t and hidden state h_{t-1}, let σ be the sigmoid function. The retaining or discarding ratio is

$$f_t = \sigma\left(W_f[h_{t-1}, x_t] + b_f\right) \tag{5}$$

where b_f is the bias at the current cell state.

Define the trained cell i_t and the corresponding cell state $\tilde{C}_t$ as

$$i_t = \sigma(W_i[h_{t-1}, x_t] + b_i), \tilde{C}_t = \tanh(W_C[h_{t-1}, x_t] + b_C). \tag{6}$$

Then updates of the cell state can be formulated as

$$C_t = f_t * C_{t-1} + i_t * \tilde{C}_t \tag{7}$$

and the calculation formula for the next hidden state is

$$h_t = \sigma(W_o[h_{t-1}, x_t] + b_o) * \tanh(C_t). \tag{8}$$

The pseudocode of the whole learning processes based on the PCA-ANN-LSTM algorithm is shown in Figure 3, where the detailed steps to detect environmental controls of soil salinity in the desert are carried out through the machine learning framework characterized in Figure 2. In order to exclude the interactions among the 12 factors, we employ partial least squares regression (PLSR) and will compare the performance of PLSR-ANN and PCA-ANN with the proposed method.

The following three indices are calculated to quantify the robustness of PCA-ANN-LSTM in previewing the possible environmental controls of soil salinity, which are also utilized in the comparison with PCA-ANN and PLSR-ANN. For a reliable comparison, the input data was uniformly divided into three subsets for all the learning processes—one for the training stage (half of the data), one for the validation stage (one-quarter of the data), and one for the testing stage (one-quarter of the data).

(1) The coefficient of determination:

$$\mathrm{RMSE} = \sqrt{\frac{\sum_i \left(y_i - y_i'\right)^2}{N}} \tag{9}$$

(2) The root-mean-square error:

$$\mathrm{R}^2 = 1 - \frac{\sum_i \left(y_i - y_i'\right)^2}{\sum_i \left(y_i - \bar{y}\right)^2} \tag{10}$$

(3) The ratio of prediction to deviation:

$$\mathrm{RPD} = \frac{\left(\sum y_i'^2 - \left[\sum \frac{y_i'^2}{n}\right] \Big/ (\mathrm{N}-1)\right)^{1/2}}{\left(\sum_i \left(y_i - y_i'\right)^2 - \left\{\left[\sum\left(y_i - y_i'\right)\right]^2 / \mathrm{N}\right\} \Big/ \mathrm{N} - 1\right)^{1/2}} \tag{11}$$

where y_i is the true value, y_i' is the predicted value, $\bar{y}$ is the average of the true value, and N is the number of environmental variables.

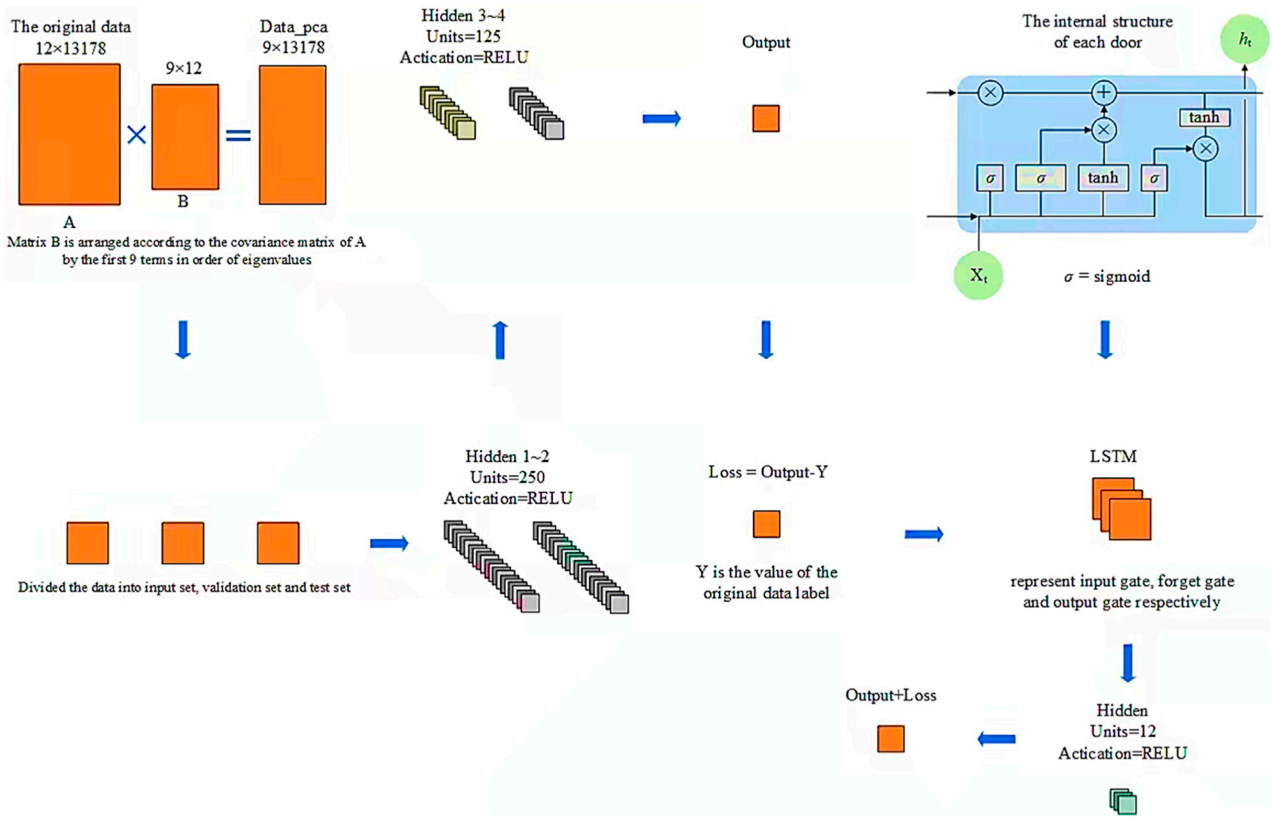

FIGURE 2
The structure diagram for detecting the potential controls.

3 Performance of the system

3.1 Efficiency of the learning processes

The contributions of twelve potential predictors to soil salinity in linear (PCA) and non-linear (ANN) relationships were determined together within a minute, implying a high efficiency of the main learning processes (LSTM only learned the errors from PCA-ANN). The learning results indicate that all the considered factors (i.e., environmental variables) can potentially influence the variation in the data of soil salinity in deserts, as shown in Figure 4. The first leading contributor is Hs and the contribution of Hs to soil salinity is 71.33%. The underlining mechanisms are easy to be understood. The status of soil salinization in deserts is restricted by the law of soil water and salt movements. Salt in soil moves with soil water—salt is transported to the surface with water in the evaporation process, and after evaporation, salt accumulates in the surface soil. The water infiltrated by rainfall in deserts can also bring salt to the deep soil layers. For a long time, there is no rainfall in the desert, the salt brought to the surface by evaporation is much more than the salt brought to the deep soils by infiltration leaching, the soil is in a salt accumulation state and salinization is aggravated.

To our surprise, Cs is the second leading contributor and its contributions to soil salinity is 13.83%. The possible mechanisms could be linked with the soil CO_2 absorption processes. Such absorption was frequently observed in deserts ecosystems and has been attributed to abiotic processes. One conjecture of these abiotic processes is that CO_2 reacts with moisture in the soil to form carbonic acid and dissolve calcium carbonate. But such reaction is not enough to explain the absorption intensity. Another conjecture is that the absorbed CO_2 has gone into deep cycles. If these conjectures were true, then soil salinity and subterranean CO_2 concentration will be linked in the reaction and deep cycles. The learning results indicated that the contribution of Cs to soil salinity is approximated to a sum of the contributions the other ten potential predictors (the sum value is 14.84%). It is also worthy to note that Ca (with a contribution=3.56%) and WS (contribution=3.77%) are also leading factors. Their contributions are almost equal and the total contribution of them two (7.33%) is approximated to the total contribution of the rest eight factors (7.51%). But some of the rest eight factors (e.g., pH) have been thought to be closely related to soil salinity. Hence, it is quite necessary to prove the robustness of the learning system, which will be done in Section 3.2.

3.2 Robustness of the learning system

The coefficient of determination (R^2), the root-mean-square error (RMSE) and the ratio of prediction to deviation (RPD) of the learning system at the training, validation, and testing stages with 200 epochs are respectively shown in Figures 5–7, and the optimized values are shown in Table 1.

The lower R^2 values of PCA-ANN at the training stage (R^2 = 0.9891), the validation stage (R^2 = 0.9844) and the testing stage (R^2 =

Input: the datasets $\boldsymbol{X} = \{\boldsymbol{x_1}, \boldsymbol{x_2}, \boldsymbol{x_3}, \dots, \boldsymbol{x_m}\}, \boldsymbol{Y}$.
Output: PCA-ANN-LSTM with a robust prediction.
Processes:
1. **For all** $\boldsymbol{x_m} \in \boldsymbol{X}$ **do**
   x_k-$\overline{x_k}$;
   end
2. Compute the matrix covMat = np.cov(meanRemoved, rowvar=0)
3. Calculate the eigenvalues and eigenvectors of the covariance matrix by SVD
4. Sort the eigenvalues from largest to smallest, select the largest k of them and respectively use the corresponding k eigenvectors as column vectors for PCA.
5. Transform the data into a new space constructed by k feature vectors.
6. Obtain the dataset $\mathbf{D} = \{(\boldsymbol{X_k}, \boldsymbol{Y_k})\}$ and set the learning rate $\boldsymbol{\eta}$ for ANN
7. Random initializes all connection weights and thresholds within (0,1)
8. Repeat
   for all $(\boldsymbol{X_k}, \boldsymbol{Y_k}) \in \mathbf{D}$ **do**
   Calculates the output of the current sample $\widehat{y_k}$ based on the current parameters and $\boldsymbol{f(x)} = \frac{\mathbf{1}}{\mathbf{1+e^{-x}}}$;
   Calculate the gradient parameter $\boldsymbol{g_J}$ of the output layer neurons ;
   Calculate the gradient parameter $\boldsymbol{e_h}$ of the hidden layer neurons;
   Update the weights $\boldsymbol{w_{hJ}}$,$\boldsymbol{v_{ih}}$ and thresholds $\boldsymbol{\theta_J}$,$\boldsymbol{\gamma_h}$ of the hidden layer to the output layer;
   end until the SVD-PCA-ANN model converges.
9. Obtain the basic results of $\boldsymbol{Y_{predict}}$ for a further correction
9. Calculate $\boldsymbol{Y_{loss}} = \boldsymbol{Y_{predict}} - \boldsymbol{Y_{true}}$
10. Construct the forgetting, input, and output gates of LSTM, respectively, which is sumarrized as $\boldsymbol{g(x)} = \boldsymbol{\sigma(\omega x + b)}$, σ=sigmoid, ω=weighting matrix, b=bias
11. Update the weights $\boldsymbol{\omega}$, $\boldsymbol{b}$ and thresholds $\boldsymbol{\theta_J}$,$\boldsymbol{\gamma_h}$ of the hidden layer to the output layer of PCA-ANN-LSTM.
12. Correct $\overline{\boldsymbol{Y}}_{\boldsymbol{loss}}$ and obtain the final predicted result $\overline{\boldsymbol{Y}}_{\boldsymbol{predict}} = \boldsymbol{Y_{predict}} + \overline{\boldsymbol{Y}}_{\boldsymbol{loss}}$

FIGURE 3
Pseudocode of the learning processes based on PCA-ANN-LSTM.

0.9764) means accurate predictions. Epochs in Figure 5 has displayed the learning processes. The learning system not only indicates a high prediction accuracy, but also indicates small errors. The RMSE values of the learning system at the training, validation, and testing stages are 0.0849, 0.1086, 0.1198, respectively. This is a degree of dispersion (not an absolute error), which further demonstrated the effectiveness of the learning system. Epochs in Figure 6 also reflect the stability of the learning system. In order to further confirm the prediction ability of the learning system, RPD is introduced to build a new emergency response process in decision-making and make up for the disadvantages of R^2 and RMSE. The RPD values of the learning system at the training, validation, and testing stages are 1.4568, 1.1042, 0.9703, respectively. This finally demonstrated the robustness of the learning system. Epochs in Figure 7 also confirm the stability of the learning system.

As a cross validation, the R^2, RMSE, RPD values were also calculated when PCA is replaced by PLSR. PLSR is also based on a linear relationship and differing from PCA, PLSR excludes the interactions among the twelve environmental factors. Performance of PLSR-ANN at the training stage (R^2 = 0.9952, RMSE = 0.0522, RPD = 2.3451), the validation stage (R^2 = 0.9922, RMSE = 0.0787, RPD = 1.4763) and the testing stage (R^2 = 0.9868, RMSE = 0.0688, RPD = 1.7906) indicate more accurate predictions. These results are a little better than the performance of PCA-ANN. The final performance of the whole system PCA-ANN-LSTM is better than both PCA-ANN and PLSR-ANN. The R^2 values of PCA-ANN-LSTM at the training, validation, and testing stages are 0.9924, 0.9931, 0.9826, respectively. The RMSE values of PCA-ANN-LSTM at the training, validation, and testing stages are 0.0123, 0.0872, 0.1079, respectively. The RPD values of PCA-ANN-LSTM at the training, validation, and testing stages are 8.282, 7.918, 6.0418, respectively. Therefore, the learning system PCA-ANN-LSTM is recommended for subsequent studies when examining potential predictors of soil salinity in deserts.

4 Discussions

Soil salinity has been widely used to describe the degree of soil salination, but in the previous studies, the dynamics of soil salinity are few linked with the CO_2 concentration above or under the ground (Singh, 2016). A series of latest studies have demonstrated abiotic soil CO_2 absorption in the alkaline land, which is closely related with salts in the soil (Chen et al., 2013). Until now, the mechanisms of such CO_2 absorption have not been fully understood. Results from the present

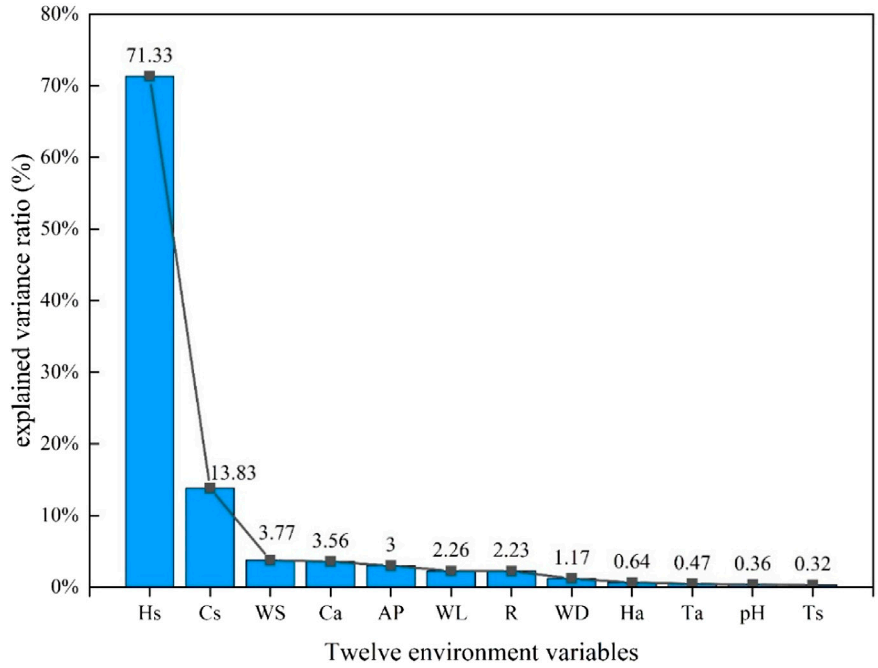

FIGURE 4
The determined contributions of twelve factors to soil salinity.

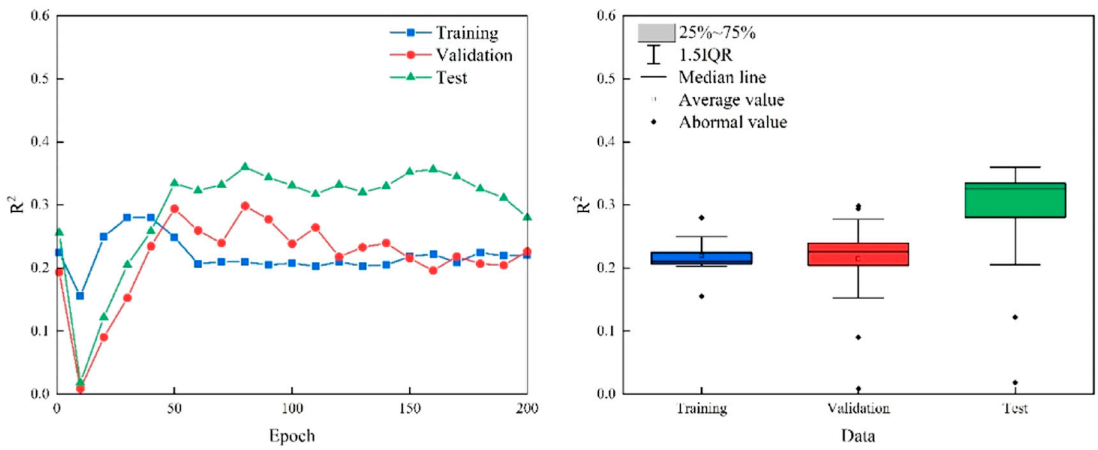

FIGURE 5
The coefficient of determination of the learning system at the training, validation, and testing stages with 200 epochs.

study indicate that subterranean CO_2 concentration and the atmospheric CO_2 concentration around the soil can both influence soil salinity in deserts. These results also present further evidences for the conjecture that the abiotic CO_2 absorption by saline-alkali soils were resulted from subterranean CO_2 sequestration in reaction of soil salts, $CO_{2,}$ and moisture.

We hence further hypothesize that the soil salination processes in deserts could be affected by such a subterranean CO_2 sequestration, since based on this new hypothesis, the underlining reaction of salts, $CO_{2,}$ and moisture in the soil would further link the dynamics of subterranean CO_2 concentration with soil salinity. Alternatively, we further hypothesize that the abiotic soil CO_2 absorption in deserts could influence the subterranean CO_2 concentration. If this hypothesis were true, the results from the learning system would be well-explained. During the reaction of salts, $CO_{2,}$ and moisture in different soil layers, soil salinity is changing (Wang et al., 2016a), where both subterranean CO_2 concentration and the atmospheric CO_2 sequestration can play significant roles. This brings new insights for reducing salination disaster. Hypothesizing that we can reduce salinization disaster through the new insights, we can mediate the subterranean CO_2 concentration through the CO_2 storage and sequestration technologies. In response to the global climate

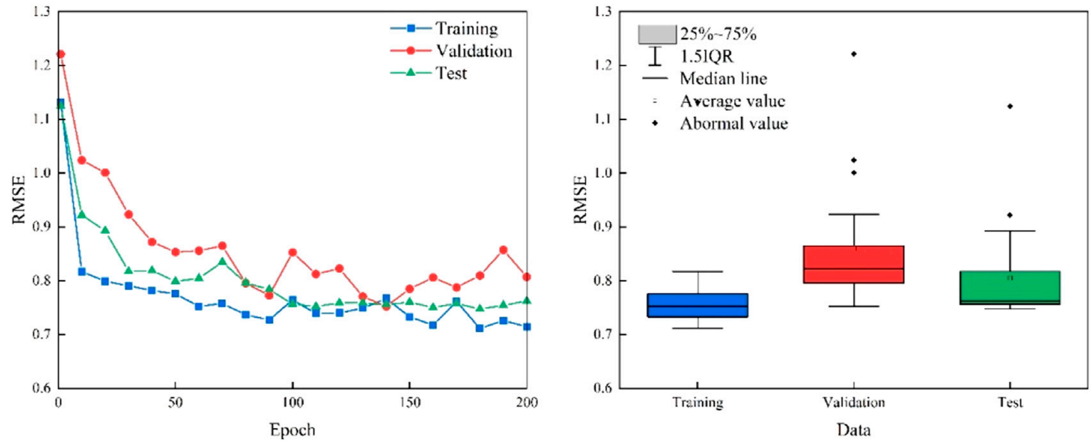

FIGURE 6
The root-mean-square error of the learning system at the training, validation, and testing stages with 200 epochs.

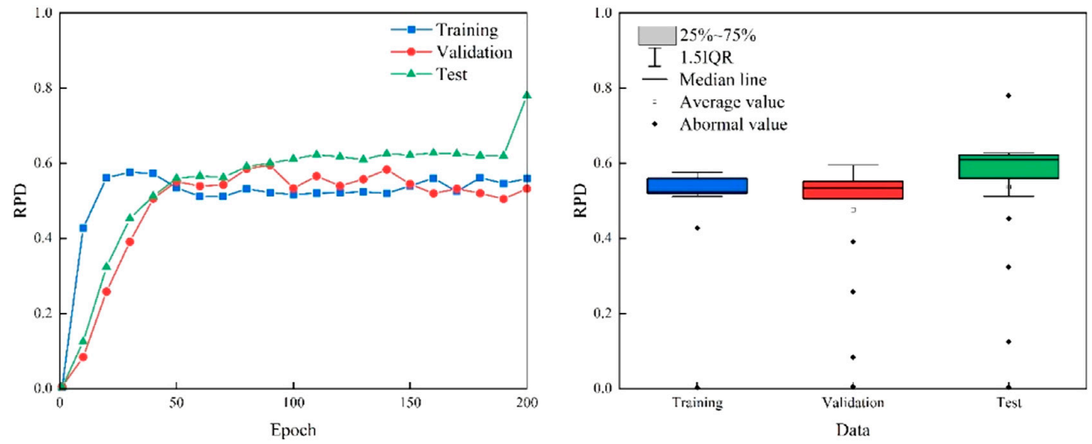

FIGURE 7
The ratio of prediction to deviation of the learning system at the training, validation, and testing stages with 200 epochs.

TABLE 1 Comparison of the SVD-PCA-ANN model with SAE, SVM, and LSTM.

Accuracy evaluation index		R^2	RMSE	RPD
Training	PLSR-ANN	0.9952	0.0522	2.3451
	PCA-ANN	0.9891	0.0849	1.4568
	PCA-ANN-LSTM	0.9924	0.0123	8.282
Validation	PLSR-ANN	0.9922	0.0787	1.4763
	PCA-ANN	0.9844	0.1086	1.1042
	PCA-ANN-LSTM	0.9931	0.0872	7.0918
Testing	PLSR-ANN	0.9868	0.0688	1.7906
	PCA-ANN	0.9764	0.1198	0.9703
	PCA-ANN-LSTM	0.9826	0.1079	6.0418

change, the world has made commitments on the peak of CO_2 emissions and the targets to achieve carbon neutrality (Chapin et al., 2006; Wang et al., 2015a). Under this goal, as an important technological approach to achieve large-scale low-carbon utilization of fossil energy, CO_2 capture, utilization and storage technology has become a hot research topic (Tapia et al., 2018). It was recognized that the geological storage potential of CO_2 is great, and the deep soil layers present the main space for CO_2 storage (Orr, 2018). Collaborating this technology with the above hypothesis, subterranean CO_2 capture, utilization and storage not only can help us to achieve carbon neutrality, but also can help us to influence the soil salinization processes.

Soil salinization and desertification are both disasters resulted from surface environmental changes, which not only depend on climate conditions, but also closely related to the role of groundwater (Amezketa, 2006). This study further links soil salinization in deserts with subterranean CO_2 concentration and advances a new hypothesis (Sunda and Cai, 2012). Since subterranean CO_2 sequestration and soil salinization process can both be influenced by the reaction of salts, CO_2, and moisture in the soil (Schlesinger, 2001), our hypothesis sounds reasonable. Nevertheless, we still need some direct evidences from isotopic analysis to further demonstrate that the soil salination processes in deserts could be affected by such a subterranean CO_2 sequestration (Inglima et al., 2009). Deserts are extremely arid areas and occupy more than 20% of the earth's land area (Chen et al., 2014). Due to high temperature, drying and strong evaporation, upwelling is the dominant process of soil water in the deserts, while the leaching and desalination processes are weak (Kowalski et al., 2008; Serrano-Ortiz et al., 2010; Sanchez-Cañete et al., 2011). These processes formed a large area of saline-alkali land in deserts and in deep soil layers around the groundwater, there are good conditions for reaction of salts, CO_2, and moisture (Stone, 2008). But there are still some outstanding questions for subsequent studies. How to assess the intensity of such reaction? How to quantify the contribution of changing processes in subterranean CO_2 concentration to the reaction? How much these processes can affect the soil salinization processes? Are these coupled processes enough to explain the apparent CO_2 absorption? If not, where has the missing CO_2 gone? Can it be attributed to some capnophiles in the deep soil layers? If these questions were appropriately addressed, then our hypothesis would be verified and make a real contribution to reduce salinization disaster in deserts.

Benefitting from the rapid development of various kinds of sensors, the subterranean processes can be further explored by different kinds of signals or images (Wang et al., 2016b). These sensors present a good base to obtain enough data for machine learning. But the mechanisms of the abiotic CO_2 absorption are still poorly understood and the soil salinity might be influenced by many other factors (Wang et al., 2015b). It is still quite necessary to integrate a series of sensors for acquiring other meteorological, soil and subterranean data. The additional data not only can present a better understanding of the whole story about soil salinization, but also can motivate researches on the effects of various environmental factors on the subterranean CO_2 concentration in other arid ecosystems and researches on the mechanisms for the abiotic soil CO_2 absorption (Rey et al., 2012; Rey, 2014; Wang et al., 2016c). Physically-based modelling (Guo et al., 2020; Medina et al., 2021) is also a next research priority.

5 Conclusion

Subterranean CO_2 concentration and the atmospheric CO_2 concentration around the soil surface can both influence soil salinity in deserts, which presents further evidence for a conjecture in the previous studies—the abiotic CO_2 absorption by saline-alkali soils in deserts were resulted from subterranean CO_2 sequestration in reaction of soil salts, CO_2, and moisture. Based on this conjecture, we advance a new hypothesis—the soil salination processes in deserts could be affected by such a subterranean CO_2 sequestration. Since the underlining reaction of salts, CO_2, and moisture in the soil would further link the dynamics of subterranean CO_2 concentration with soil salinity. Due to strong water-salt processes in deserts, the water in the deep soil layers move upward [resp. downward] in the dry season [resp. the rainy season], and then react with salts and CO_2 in the capillary. The story sounds well. But we need further evidences. A better understanding of the whole story is still quite necessary.

Data availability statement

The raw data supporting the conclusion of this article will be made available by the authors, without undue reservation.

Author contributions

PA and WW were mainly responsible for data collection, code convenience and paper writing as the core contributor of this paper. ZZ and LC assisted in the completion of experiments and data table compilation. WW led the project and conceive the main idea of this research. CX was responsible for the guidance of the experimental code and the language polishing of the paper.

Funding

This research was funded by the Ningbo Natural Science Foundation (2019A610106), the Strategic Priority Research Program of Chinese Academy of Sciences (XDA20060303), the National Natural Science Foundation of China (41571299) and the High-level Base-building Project for Industrial Technology Innovation (1021GN204005-A06).

Conflict of interest

The authors declare that the research was conducted in the absence of any commercial or financial relationships that could be construed as a potential conflict of interest.

Publisher's note

References

Ahmad, T., and Zhang, D. (2022). A data-driven deep sequence-to-sequence long-short memory method along with a gated recurrent neural network for wind power forecasting. *Energy* 239, 122109. doi:10.1016/j.energy.2021.122109

Ali, G., Ali, T., Irfan, M., Draz, U., Sohail, M., Glowacz, A., et al. (2020). IoT based smart parking system using deep long short memory network. *Electronics* 9 (10), 1696. doi:10.3390/electronics9101696

Amezketa, E. (2006). An integrated methodology for assessing soil salinization, a pre-condition for land desertification. *J. Arid Environ.* 67 (4), 594–606. doi:10.1016/j.jaridenv.2006.03.010

Aragüés, R., Medina, E. T., Zribi, W., Claveria, I., Alvaro-Fuentes, J., and Faci, J. (2015). Soil salinization as a threat to the sustainability of deficit irrigation under present and expected climate change scenarios. *Irrigation Sci.* 33 (1), 67–79. doi:10.1007/s00271-014-0449-x

Bouksila, F., Bahri, A., Berndtsson, R., Persson, M., Rozema, J., and Van der Zee, S. E. (2013). Assessment of soil salinization risks under irrigation with brackish water in semiarid Tunisia. *Environ. Exp. Bot.* 92, 176–185. doi:10.1016/j.envexpbot.2012.06.002

Chahal, A., and Gulia, P. (2019). Machine learning and deep learning. *Int. J. Innovative Technol. Explor. Eng.* 8 (12), 4910–4914. doi:10.35940/ijitee.l3550.1081219

Chang, Z. L., Du, Z., Zhang, F., Huang, F., Chen, J., Li, W., et al. (2020). Landslide susceptibility prediction based on Remote sensing images and GIS: Comparisons of supervised and unsupervised machine learning models. *Remote Sens.* 12 (3), 502. doi:10.3390/rs12030502

Chapin, F. S., Woodwell, G. M., Randerson, J. T., Rastetter, E. B., Lovett, G. M., Baldocchi, D. D., et al. (2006). Reconciling carbon-cycle concepts, terminology, and methods. *Ecosystems* 9 (7), 1041–1050. doi:10.1007/s10021-005-0105-7

Chen, X., Wang, W. F., Luo, G. P., Li, L. H., and Li, Y. (2013). Time lag between carbon dioxide influx to and efflux from bare saline-alkali soil detected by the explicit partitioning and reconciling of soil CO_2 flux. *Stoch. Environ. Res. Risk Assess.* 27 (3), 737–745. doi:10.1007/s00477-012-0636-3

Chen, X., Wang, W. F., Luo, G. P., and Ye, H. (2014). Can soil respiration estimate neglect the contribution of abiotic exchange? *J. Arid Land* 6 (2), 129–135. doi:10.1007/s40333-013-0244-1

Coşkun, M., Yildirim, Ö., Ayşegül, U., and Demir, Y. (2017). An overview of popular deep learning methods[J]. *Eur. J. Tech.* 7 (2), 165–176. doi:10.23884/ejt.2017.7.2.11

De Pascale, S., Maggio, A., and Barbieri, G. (2005). Soil salinization affects growth, yield and mineral composition of cauliflower and broccoli. *Eur. J. Agron.* 23 (3), 254–264. doi:10.1016/j.eja.2004.11.007

Dehaan, R. L., and Taylor, G. R. (2002). Field-derived spectra of salinized soils and vegetation as indicators of irrigation-induced soil salinization. *Remote Sens. Environ.* 80 (3), 406–417. doi:10.1016/s0034-4257(01)00321-2

Ding, J. L., Wu, M. C., and Tiyip, T. (2011). Study on soil salinization information in arid region using Remote sensing technique. *Agric. Sci. China* 10 (3), 404–411. doi:10.1016/s1671-2927(11)60019-9

El Harti, A., Lhissou, R., Chokmani, K., Ouzemou, J. e., Hassouna, M., Bachaoui, E. M., et al. (2016). Spatiotemporal monitoring of soil salinization in irrigated Tadla Plain (Morocco) using satellite spectral indices. *Int. J. Appl. Earth Observation Geoinformation* 50, 64–73. doi:10.1016/j.jag.2016.03.008

Gao, S. (2022). A two-channel attention mechanism-based mobileNetV2 and bidirectional long short memory network for multi-modal dimension dance emotion recognition[J]. *J. Appl. Sci. Eng.* 26 (4), 455–464.

Gatos, I., Tsantis, S., Spiliopoulos, S., Karnabatidis, D., Theotokas, I., Zoumpoulis, P., et al. (2019). Temporal stability assessment in shear wave elasticity images validated by deep learning neural network for chronic liver disease fibrosis stage assessment. *Med. Phys.* 46 (5), 2298–2309. doi:10.1002/mp.13521

Ghollarata, M., and Raiesi, F. (2007). The adverse effects of soil salinization on the growth of Trifolium alexandrinum L. and associated microbial and biochemical properties in a soil from Iran. *Soil Biol. Biochem.* 39 (7), 1699–1702. doi:10.1016/j.soilbio.2007.01.024

Gorgij, A. D., Askari, G., Taghipour, A. A., Jami, M., and Mirfardi, M. (2023). Spatiotemporal forecasting of the groundwater quality for irrigation purposes, using deep learning method: Long short-term memory (LSTM). *Agric. Water Manag.* 277, 108088. doi:10.1016/j.agwat.2022.108088

Gu, Q., Lu, N., and Liu, L. (2019). A novel recurrent neural network algorithm with long short-term memory model for futures trading. *J. Intelligent Fuzzy Syst.* 37 (4), 4477–4484. doi:10.3233/jifs-179280

Guo, Z. Z., Chen, L. X., Gui, L., Du, J., Yin, K., and Do, H. M. (2020). Landslide displacement prediction based on variational mode decomposition and WA-GWO-BP model. *Landslides* 17, 567–583. doi:10.1007/s10346-019-01314-4

Hao, X., Zhang, G., and Ma, S. (2016). Deep learning. *Int. J. Semantic Comput.* 10 (03), 417–439. doi:10.1142/s1793351x16500045

Hassani, A., Azapagic, A., and Shokri, N. (2021). Global predictions of primary soil salinization under changing climate in the 21st century[J]. *Nat. Commun.* 12 (1), 1–17.

Huang, F., Li, Z. X., Xiang, S. C., and Wang, R. (2021). A new wind power forecasting algorithm based on long short-term memory neural network[J]. *Int. Trans. Electr. Energy Syst.* 31 (12), e13233.

Huang, F. M., Cao, Z. S., Guo, J. F., Jiang, S. H., Li, S., and Guo, Z. Z. (2020). Comparisons of heuristic, general statistical and machine learning models for landslide susceptibility prediction and mapping. *Catena* 191, 104580. doi:10.1016/j.catena.2020.104580

Huang, F. M., Cao, Z. S., Jiang, S. H., Zhou, C., Huang, J., and Guo, Z. (2020). Landslide susceptibility prediction based on a semi-supervised multiple-layer perceptron model. *Landslides* 17, 2919–2930. doi:10.1007/s10346-020-01473-9

Huang, F. M., Zhang, J., Zhou, C. B., Wang, Y. H., Huang, J. S., Zhu, L., et al. (2020). A deep learning algorithm using a fully connected sparse autoencoder neural network for landslide susceptibility prediction[J]. *Landslides* 17 (01), 217~229.

Inglima, I., Alberti, G., Bertolini, T., Vaccari, F. P., Gioli, B., Miglietta, F., et al. (2009). Precipitation pulses enhance respiration of mediterranean ecosystems: The balance between organic and inorganic components of increased soil CO_2 efflux[J]. *Glob. Change Biol.* 15 (5), 1289–1301. doi:10.1111/j.1365-2486.2008.01793.x

Jesus, J., Castro, F., Niemelä, A., Borges, M. T., and Danko, A. S. (2015). Evaluation of the impact of different soil salinization processes on organic and mineral soils[J]. *Water, Air, & Soil Pollut.* 226 (4), 1–12.

Jiang, S. H., Huang, J., Huang, F. M., Yang, J. H., Yao, C., and Zhou, C. B. (2018). Modelling of spatial variability of soil undrained shear strength by conditional random fields for slope reliability analysis [J]. *Appl. Math. Model.* 63, 374~389.

Kato, N., Fadlullah, Z. M., Mao, B., Tang, F., Akashi, O., Inoue, T., et al. (2016). The deep learning vision for heterogeneous network traffic control: Proposal, challenges, and future perspective. *IEEE Wirel. Commun.* 24 (3), 146–153. doi:10.1109/mwc.2016.1600317wc

Klema, V., and Laub, A. (1980). The singular value decomposition: Its computation and some applications. *IEEE Trans. automatic control* 25 (2), 164–176. doi:10.1109/tac.1980.1102314

Klimov, V., Balandina, A., and Chernyshov, A. (2020). Application of long-short memory neural networks in semantic search engines development. *Procedia Comput. Sci.* 169, 388–392. doi:10.1016/j.procs.2020.02.234

Kotb, T. H. S., Watanabe, T., Ogino, Y., and Tanji, K. K. (2000). Soil salinization in the Nile Delta and related policy issues in Egypt. *Agric. water Manag.* 43 (2), 239–261. doi:10.1016/s0378-3774(99)00052-9

Kowalski, A. S., Serrano-Ortiz, P., Janssens, I. A., Sanchez-Moral, S., Cuezva, S., Domingo, F., et al. (2008). Can flux tower research neglect geochemical CO_2 exchange? *Agric. For. Meteorology* 148 (148), 1045–1054. doi:10.1016/j.agrformet.2008.02.004

Lavado, R. S., and Taboada, M. A. (1987). Soil salinization as an effect of grazing in a native grassland soil in the Flooding Pampa of Argentina. *Soil Use Manag.* 3 (4), 143–148. doi:10.1111/j.1475-2743.1987.tb00724.x

LeCun, Y., Bengio, Y., and Hinton, G. (2015). Deep learning. *Nature* 521 (7553), 436–444. doi:10.1038/nature14539

Li, J., Pu, L., Han, M., Zhu, M., Zhang, R., and Xiang, Y. (2014). Soil salinization research in China: Advances and prospects. *J. Geogr. Sci.* 24 (5), 943–960. doi:10.1007/s11442-014-1130-2

Li, N., Chang, F., and Liu, C. (2022). Human-related anomalous event detection via spatial-temporal graph convolutional autoencoder with embedded long short-term memory network. *Neurocomputing* 490, 482–494. doi:10.1016/j.neucom.2021.12.023

Li, P., Qian, H., and Wu, J. (2018). Conjunctive use of groundwater and surface water to reduce soil salinization in the Yinchuan Plain, North-West China. *Int. J. Water Resour. Dev.* 34 (3), 337–353. doi:10.1080/07900627.2018.1443059

Li-Xian, Y., Guo-Liang, L., Shi-Hua, T., Gavin, S., and Zhao-Huan, H. (2007). Salinity of animal manure and potential risk of secondary soil salinization through successive manure application. *Sci. total Environ.* 383 (1-3), 106–114. doi:10.1016/j.scitotenv.2007.05.027

Mandel, J. (1982). Use of the singular value decomposition in regression analysis. *Am. Statistician* 36 (1), 15–24. doi:10.2307/2684086

Medina, V., Hürlimann, M., Guo, Z. Z., Lloret, A., and Vaunat, J. (2021). Fast physically-based model for rainfall-induced landslide susceptibility assessment at regional scale. *Catena* 201, 105213. doi:10.1016/j.catena.2021.105213

Metternicht, G., and Zinck, A. (2008). *Remote sensing of soil salinization: Impact on land management [M]*. FL, United States: CRC Press.

Nachshon, U. (2018). Cropland soil salinization and associated hydrology: Trends, processes and examples. *Water* 10 (8), 1030. doi:10.3390/w10081030

O'Doherty, J. E., Lebedev, M. A., Ifft, P. J., Zhuang, K. Z., Shokur, S., Bleuler, H., et al. (2011). Active tactile exploration using a brain–machine–brain interface. *Nature* 479 (7372), 228–231. doi:10.1038/nature10489

Okur, B., and Örçen, N. (2020). *Soil salinization and climate change[M]*. Elsevier.

Orr, F. M. (2018). Carbon capture, utilization, and storage: An update. *Spe J.* 23 (06), 2444–2455. doi:10.2118/194190-pa

Paige, C. C., and Saunders, M. A. (1981). Towards a generalized singular value decomposition. *SIAM J. Numer. Analysis* 18 (3), 398–405. doi:10.1137/0718026

Rengasamy, P. (2016). *Soil salinization[M]*. Oxford: Oxford Research Encyclopedia of Environmental Science.

Rey, A., Belelli-Marchesini, L., Were, A., Serrano-ortiz, P., Etiope, G., Papale, D., et al. (2012). Wind as a main driver of the net ecosystem carbon balance of a semiarid Mediterranean steppe in the South East of Spain. *Glob. Change Biol.* 18 (2), 539–554. doi:10.1111/j.1365-2486.2011.02534.x

Rey, A. (2014). Mind the gap: Non-biological processes contributing to soil CO_2 efflux. *Glob. Change Biol.* 21 (5), 1752–1761. doi:10.1111/gcb.12821

Robinson, P. M., and Zaffaroni, P. (1997). Modelling nonlinearity and long memory in time series[J]. *Fields Inst. Commun.* 11, 161–170.

Rusnac, A. L., and Grigore, O. (2022). Imaginary speech recognition using a convolutional network with long-short memory. *Appl. Sci.* 12 (22), 11873. doi:10.3390/app122211873

Salman, A. G., Heryadi, Y., Abdurahman, E., and Suparta, W. (2018). Single layer & multi-layer long short-term memory (LSTM) model with intermediate variables for weather forecasting. *Procedia Comput. Sci.* 135, 89–98. doi:10.1016/j.procs.2018.08.153

Sanchez-Cañete, E. P., Serrano-Ortiz, P., Kowalski, A. S., Oyonarte, C., and Domingo, F. (2011). Subterranean CO_2 ventilation and its role in the net ecosystem carbon balance of a karstic shrubland. *Geophys. Res. Lett.* 38 (9), 159–164.

Savich, V. I., Artikova, H. T., Nafetdinov, S. S., and Salimova, K. H. (2021). Optimization of plant development in case of soil salinization. *Am. J. Agric. Biomed. Eng.* 3 (02), 24–29. doi:10.37547/tajabe/volume03issue02-05

Schlesinger, W. H. (2001). Carbon sequestration in soils: Some cautions amidst optimism. *Agric. Ecosyst. Environ.* 82 (1-3), 121–127. doi:10.1016/s0167-8809(00)00221-8

Schofield, R., Thomas, D. S. G., and Kirkby, M. J. (2001). Causal processes of soil salinization in Tunisia, Spain and Hungary. *Land Degrad. Dev.* 12 (2), 163–181. doi:10.1002/ldr.446

Serrano-Ortiz, P., Roland, M., Sanchez-Moral, S., Janssens, I. A., Domingo, F., Godderis, Y., et al. (2010). Hidden, abiotic CO_2 flows and gaseous reservoirs in the terrestrial carbon cycle: Review and perspectives. *Agric. For. Meteorology* 151 (4), 321–329. doi:10.1016/j.agrformet.2010.01.002

Singh, A. (2015). Soil salinization and waterlogging: A threat to environment and agricultural sustainability. *Ecol. Indic.* 57, 128–130. doi:10.1016/j.ecolind.2015.04.027

Singh, K. (2016). Microbial and enzyme activities of saline and sodic soils. *Land Degrad. Dev.* 27 (3), 706–718. doi:10.1002/ldr.2385

Skrede, O. J., De Raedt, S., Kleppe, A., Hveem, T. S., Liestol, K., Maddison, J., et al. (2020). Deep learning for prediction of colorectal cancer outcome: A discovery and validation study. *Lancet* 395 (10221), 350–360. doi:10.1016/s0140-6736(19)32998-8

Stewart, G. W. (1993). On the early history of the singular value decomposition. *SIAM Rev.* 35 (4), 551–566. doi:10.1137/1035134

Stone, R. (2008). Have Desert researchers discovered a hidden loop in the carbon cycle? *Science* 320 (5882), 1409–1410. doi:10.1126/science.320.5882.1409

Sunda, W. G., and Cai, W. J. (2012). Eutrophication induced CO_2-acidification of subsurface coastal waters: Interactive effects of temperature, salinity, and atmospheric pCO_2[J]. *Environ. Sci. Technol.* 46 (19), 10651–10659. doi:10.1021/es300626f

Tapia, J. F. D., Lee, J. Y., Ooi, R. E. H., Foo, D. C., and Tan, R. R. (2018). A review of optimization and decision-making models for the planning of CO_2 capture, utilization and storage (CCUS) systems[J]. *Sustain. Prod. Consum.* 13, 1–15. doi:10.1016/j.spc.2017.10.001

Teh, S. Y., and Koh, H. L. (2016). Climate change and soil salinization: Impact on agriculture, water and food security[J]. *Int. J. Agric. For. Plant.* 2, 1–9.

Tian, C. Y., and Zhou, H. F. (2000). The proposal on control of soil salinization and agricultural sustainable development in the 21st century in Xinjian[J]. *Arid. Land Geogr.* 23 (2), 177–181.

Van Loan, C. F. (1976). Generalizing the singular value decomposition. *SIAM J. Numer. Analysis* 13 (1), 76–83. doi:10.1137/0713009

Wang, W. F., Cai, H. J., Deng, X. Y., and Zhang, L. M. (2021). *Interdisciplinary evolution of the machine brain: Vision*. Touch & Minds [M]Springer.

Wang, W. F., Chen, X., and Yao, T. Z. (2022). *Five-layer intelligence of the machine brain: System modelling and simulation [M]*. Springer.

Wang, W. F., Deng, X. Y., Ding, L., and Zhang, L. M. (2020). *Brain-inspired intelligence and visual perception [M]*. Springer.

Wang, W. F., Chen, X., and Pu, Z. (2015). Negative soil respiration fluxes in unneglectable arid regions. *Pol. J. Environ. Stud.* 24 (2), 905–908. doi:10.15244/pjoes/23878

Wang, W. F., Chen, X., Wang, L., Zhang, H., Yin, G., and Zhang, Y. (2016). Approaching the truth of the missing carbon sink. *Pol. J. Environ. Stud.* 25 (4), 1799–1802. doi:10.15244/pjoes/62357

Wang, W. F., Chen, X., Zhang, H., Jing, C., Zhang, Y., and Yan, B. (2015). Highlighting photocatalytic H_2-production from natural seawater and the utilization of quasi-photosynthetic absorption as two ultimate solutions for CO_2 mitigation. *Int. J. Photoenergy* 2015, 1–11. doi:10.1155/2015/481624

Wang, W. F., Chen, X., Zhang, H. W., Lv, Z. H., Liu, Z., Qian, J., et al. (2016). *Intelligence in ecology: How internet of things expands insights into the missing CO_2 sink*. Scientific Programming. Article ID: 589723.

Wang, W. F., Chen, X., Zhang, Y. F., Yu, J., Ma, T., Lv, Z., et al. (2016). Nanodeserts: A conjecture in nanotechnology to enhance quasi-photosynthetic CO2 absorption. *Int. J. Polym. Sci.* 2016, 1–10. doi:10.1155/2016/5027879

Wang, Y., and Li, Y. (2013). Land exploitation resulting in soil salinization in a desert–oasis ecotone. *Catena* 100, 50–56. doi:10.1016/j.catena.2012.08.005

Wang, Z., Fan, B., and Guo, L. (2019). Soil salinization after long-term mulched drip irrigation poses a potential risk to agricultural sustainability. *Eur. J. Soil Sci.* 70 (1), 20–24. doi:10.1111/ejss.12742

Welle, P. D., and Mauter, M. S. (2017). High-resolution model for estimating the economic and policy implications of agricultural soil salinization in California. *Environ. Res. Lett.* 12 (9), 094010. doi:10.1088/1748-9326/aa848e

Wu, J. H., Li, P. Y., Qian, H., and Fang, Y. (2014). Assessment of soil salinization based on a low-cost method and its influencing factors in a semi-arid agricultural area, northwest China. *Environ. Earth Sci.* 71 (8), 3465–3475. doi:10.1007/s12665-013-2736-x

Xiaohou, S., Min, T., Ping, J., and Weiling, C. (2008). Effect of EM Bokashi application on control of secondary soil salinization[J]. *Water Sci. Eng.* 1 (4), 99–106.

Yang, C., Wang, X., Miao, F., Li, Z., Tang, W., and Sun, J. (2020). Assessing the effect of soil salinization on soil microbial respiration and diversities under incubation conditions. *Appl. Soil Ecol.* 155, 103671. doi:10.1016/j.apsoil.2020.103671

Zhou, M., Butterbach-Bahl, K., Vereecken, H., and Brüggemann , N. (2017). A meta-analysis of soil salinization effects on nitrogen pools, cycles and fluxes in coastal ecosystems. *Glob. change Biol.* 23 (3), 1338–1352. doi:10.1111/gcb.13430

Zhuang, Q., Shao, Z., Li, D., Huang, X., Cai, B., Altan, O., et al. (2022). Unequal weakening of urbanization and soil salinization on vegetation production capacity. *Geoderma* 411, 115712. doi:10.1016/j.geoderma.2022.115712

Zhuang, Z. K., Li, X. Q., Wang, W. F., and Chen, X. (2021). Examining the potential environmental controls of underground CO_2 concentration in arid regions by an SVD-PCA-ANN preview model [J]. *Math. Problems Eng.* 2021, 1–8. doi:10.1155/2021/9840335